



Characterization and identification of organic molecules in thermal desalination plant scale

Troy N. Green^{a,*}, Nouri Hassan^b, Nagmeddin Elwaer^b, Christopher Fellows^{a,c}, Abdelkader Meroufel^a, Abdullah Al-Mayouf^b, Syed Ali^b

^aSWCC: Desalination Technologies Research Institute (DTRI), Saudi Arabia, Tel. +96613 3430333 Ext. 31715; emails: TGreen@swcc.gov.sa (T.N. Green), CMichael@swcc.gov.sa (C. Fellows), Tel. +46 730472263; email: Nabil_Wahran@hotmail.fr (A. Meroufel)

^bSABIC: Analytical Laboratories (KSA Analytical), Saudi Arabia, Tel. +96611 4999815; email: Hassannm@sabic.com (N. Hassan), Tel. +96611 4999787; email: Elwaern@sabic.com (N. Elwaer), Tel. +966114999752; email: Mayoufam@sabic.com (A. Al-Mayouf), Tel. +91 7310612158; email: Alisyed156@yahoo.com (S. Ali)

^cThe University of New England: School of Science and Technology, Australia

Received 12 November 2019; Accepted 12 July 2020

ABSTRACT

Scale samples from a 144,000 m³/d Arabian Gulf multi-stage flash (MSF) desalination plant were collected and assayed for organic, biological, and inorganic compounds. Samples were collected from the bottom side of the deaerator and the first flash chamber of a 24,000 m³/d MSF unit. For the first time, organic compounds and adenosine triphosphate were characterized and identified in both selected locations. Within predominantly calcium carbonate (in the deaerator) and magnesium hydroxide (in the first stage of MSF) scale samples, organics were detected, and their potential sources suggested based on related literature. Organic compounds found are consistent with degradation components of bacterioneuston with some contribution from species present in the seawater source and pretreatment chemicals. These findings raise the possibility of a significant role of organic compounds in alkaline scale nucleation and growth in the MSF process.

Keywords: Scale; Organics; Adenosine triphosphate (ATP); Kinetics; Calcium carbonate; Magnesium hydroxide

1. Introduction

The two primary processes for desalination of seawater to potable water are membrane and thermal-based. While seawater reverse osmosis (SWRO) is more energy efficient with less CAPEX and OPEX per cubic meter of production [1] (than stand-alone thermal technologies); it is highly sensitive to environmental seawater changes. Changes in seawater conditions require expensive physical and chemical pretreatments that alter bioactivity of feed water, enhancing biofouling and biodegradation of process structures and membranes. The application of SWRO is growing, but

there remains a large installed capacity of thermal desalination technologies. The use of renewable energy applications is helping to reduce thermal OPEX and water production costs. However, thermal desalination processes remain energy-intensive. The significant advantage of thermal vs. SWRO, with regards to water security, is robustness in production under most environmental changes of the sea, such as red tides, algal blooms, and jellyfish outbreaks. However, like SWRO, thermal multi-stage flash (MSF) plants are also susceptible to industrial process fouling.

The MSF process desalts seawater by flashing a portion of the water into steam in multiple stages under vacuum.

* Corresponding author.

Produced vapor is condensed into fresh water on the tubular exchanger at the top of the stage. The system includes three major sections: the brine heater, heat recovery, and the heat rejection sections. The brine heater drives the flashing process by heating the recycled brine stream to top brine temperature which is an essential design parameter. The concentration of circulating brine is adjusted through the continuous addition of deaerated seawater make-up to avoid high levels of undesirable scale. Further details on the MSF process can be found in journal publications.

Fouling in thermal desalination plants is mostly due to scale formation in deaerators, flash chambers, heat transfer surfaces, and water boxes. At elevated temperatures, salts such as calcium carbonate (CaCO_3), calcium sulfate (CaSO_4), and magnesium hydroxide ($\text{Mg}(\text{OH})_2$) experience inverse solubility (retro-saturation). Retro-saturation results when the addition of heat to a solvent causes an endothermic impact on solutes (Le Châtelier principle) driving equilibrium in favor of reactants (agglomeration of salts) [2]. The two main components of the alkaline scale formed in thermal desalination processes below 100°C are the inverse solubility salts of calcium carbonate (CaCO_3) and magnesium hydroxide ($\text{Mg}(\text{OH})_2$). These salts arise from the decomposition of the hydrogen carbonate ion (HCO_3^-), Fig. 1 [3]. Depending on temperature and pH, hydrogen carbonate may decompose either to carbonate (CO_3^{2-}) or hydroxide (OH^-), as shown in Fig. 1. In the presence of calcium, the formation of calcium carbonate is preferred between 65°C and 80°C , above which temperature $\text{Mg}(\text{OH})_2$ dominates [4].

A thermodynamic explanation of CaCO_3 and $\text{Mg}(\text{OH})_2$ formation, in desalination conditions, based on Gibbs free energy, is presented by Alhamzah and Fellows [3]. In Fig. 1, the variation of calculated Gibbs free energy ($\Delta G^\circ_{\text{rxn}}$) associated with calcium carbonate and magnesium hydroxide scale formation (between 25°C and 100°C of brine solution, concentration factor (CF) = 1.4, $[\text{HCO}_3^-] = 160$ ppm, pH 9.0), is proposed. Conclusions of Alhamzah and Fellows [3] are consistent with the findings of Shams El Din and Mohammed [4].

Gibb's free energy gives insight into the favorability of reactants to the product or vice versa depending on negative or positive ΔG° value, respectively. However, ΔG° does

not explain scale nucleation or growth. Nucleation and scale growth are best understood through reaction kinetics. This concept was introduced by Hasson [5]. Since then, authors have tried to study the kinetics of scale, especially in oil field conditions, which is close to thermal desalination. Among them, Dawe and Zhang [6] researched calcium carbonate precipitation using visual observation within a glass micro-model. The authors could determine the crystal growth rate depending on temperature, ionic strength, and activation energy. Similarly, Østvold and Randhol [7] included the effect of sand presence, which was found to enhance the calcium carbonate precipitation rate by reducing the induction time. Introducing kinetics allows for a mechanistic understanding of scale formation and growth by dissecting triggers that may impact rates of reactions.

Inverse solubility salts can nucleate either on interfaces (giving scale formation directly) or form suspensions (that precipitate on surfaces). The presence of organics in the matrix has been shown to slow down the rates of scale formation, increasing the supersaturation of a solution [8]. In a closed system, nucleation leading to growth can produce scale artifacts of different types and sizes. Scale formation proceeds until a shift in concentration gradient limits growth.

In an open system, scale formation continues because the replenishment of bulk solution is continuous, and fluid saturation is maintained. Due to organics in the bulk solution, rates of scale growth are slowed, resulting in uniform scale distribution of similar shape and size [9]. Flashing in thermal desalination systems may increase rates of scale growth with the same form and size distribution in the flash chamber.

The most significant adverse effect of scale growth is a reduction in heat transfer coefficient caused by deposition of salts with low thermal conductivity on metal surfaces—resulting in losses of energy and production. The low thermal conductivity of scale can also create areas of heat nucleation on metal surfaces, raising the temperature to over $1^\circ\text{C}/0.03$ mm of oxide build-up, causing tube stress and damage [10]. Within heat exchangers, scale formation may also impact water production by blocking demisters in flash chambers.

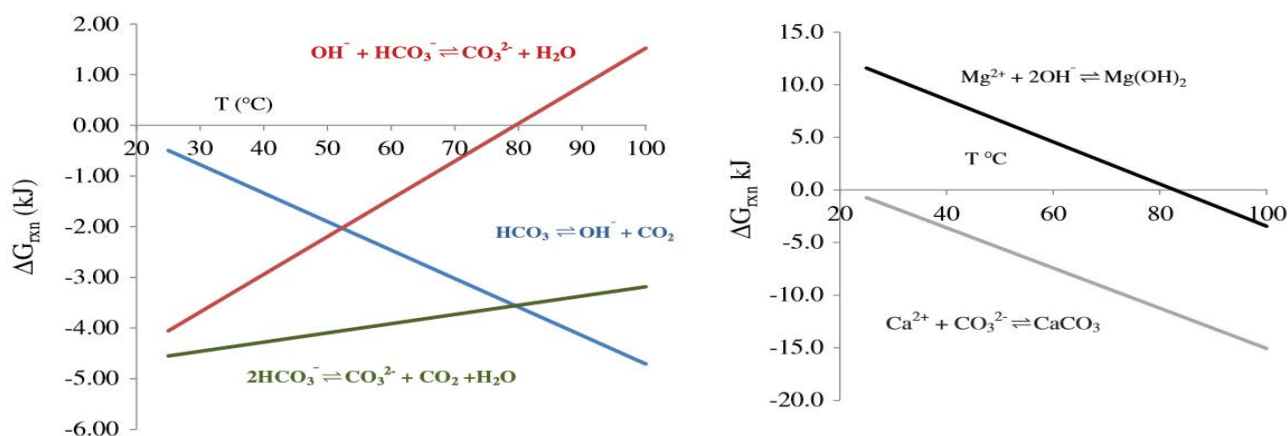


Fig. 1. Thermodynamics of the formation of (a) calcium carbonate and (b) magnesium hydroxide in thermal desalination.

Much is known about the effects of scale on thermal desalination processes and structures. However, little is known about the organic compounds associated with scale foulants. This may arise from a lack of methods for micro-extraction and analysis of mineral species and organic compounds or a lack of interest arising from the preconception that the predominant component of a scale is sufficient to define its form and properties.

In this work, experimental methods developed for organic and trace metal analysis of scale were applied to scale collected from deaerators and the first flash chamber of an MSF distiller from a Plant located on the Arabian Gulf coast of Saudi Arabia. The location of the plant has high ambient water quality conditions-Table 1 [11], warranting an in-depth investigation of potential organic intercalates associated with scale.

2. Methods

Samples collected from the deaerator and the first flash chamber of a commercial MSF unit were transferred to sterile zip-lock plastic bags and processed using mallet pulverization. Pulverized samples were thoroughly mixed and homogenized before air-drying (in a fume hood at room temperature for 3 h). Precisely, 2.0 g of the sample material was placed in a crucible and loaded into the LECO TGA 701 furnace for loss on ignition (LOI) determination (LECO Corporation, 3000 Lakeview Avenue, St. Joseph, MI 49085). Following LOI analysis, samples were cooled and placed in a desiccator. Dehydrating is essential for accurate determination of sample weight when mixed with borate flux.

2.1. Fusion preparation

In preparation for fusion, 1.0 g of the LOI samples were weighed in a 95% Pt – 5% Au crucible. Then, 6.0 g of 49.75% lithium metaborate, 49.75% lithium tetraborate, and 0.50% lithium iodide flux mixture was added to the sample (from the same crucible). Sample and flux were thoroughly mixed (in the crucible) and mounted on the THEOX electrical fusion machine (Claisse Canada). A borate mixture was chosen because it is an excellent solvent for oxides produced from LOI analysis when heated.

Table 1
Water quality and biological parameters for Arabian Gulf waters

Parameters	Ambient concentrations (range)
Salinity (mS/cm)	52.90–58.27
Temperature (°C)	18–35
Total suspended solids (mg/L)	1.20–16.00
pH	8.10–8.60
Dissolved oxygen (mg/L)	4.74–6.69
Dry weight density (mg/L)	0.02–162.16
Plankton density (cells/m ³)	
Diatoms	1.01E+05–4.25E+07
Dinoflagellates	2.45E+04–3.25E+05
Cyanobacteria	2.93E+04–2.47E+05

Furthermore, the 0.50% lithium iodide in the borate flux prevented fluxed samples from adhering to crucibles. Platinum crucibles were chosen for the fusion because of strength and durability upon heating. Crucibles cool quickly and are made from a metal undetectable in sample analyses.

Fusing and agitation were carried out automatically using a THEOX electrical fusion machine-applying a seven steps temperature program (Fig. 2). Both fusing and agitation steps were carried out at 1,150°C for 18 min (to ensure that glass beads were homogenous with samples, and there were no inclusions within the mixture). Upon program completion, the sample was poured into a platinum casting plate and cooled for 4 min. Beads were checked for cracking, and irregularities then labeled and placed onto an X-ray fluorescence (XRF) spectrometer for analysis.

2.2. X-ray fluorescence

Samples were analyzed using a wavelength dispersive X-ray fluorescence (WD-XRF) spectrometer (Bruker AXS S8 TIGER, Bruker AXS GmbH, Ostliche Rheinbrückenstr. 49, 76187 Karlsruhe, Germany) equipped with; an end window X-ray tube (with Rh-target), a ten-position beam filter changer, two different detectors and four analyzer crystals (OVO-B OVO-55, LiF 200 and polyethylene terephthalate). Oxide values in the prepared glass beads were determined by the standard test method (using the best detection program).

2.3. Scanning electron microscopy

Particles of scale were placed on 12.5 mm diameter aluminum scanning electron microscopy (SEM) stubs having sticky 12 mm diameter carbon tabs. Samples were viewed by a Quanta 200 SEM (Field Electron and Ion Company, Achtseweg Noord 5, 5651 GG Eindhoven, Netherlands) with an accelerating voltage of 20.0 kV, at a working distance of 10 mm, and a spot size of 4.5. Images were digitally recorded in secondary electron imaging mode at different magnifications. Energy-dispersive X-ray spectroscopy (EDX) analysis was performed on multiple spots using an EDAX Genesis XM4 system attached to SEM (EDAX Corporate Headquarters EDAX, LLC, 91 McKee Drive, Mahwah, NJ 07430 U.S.A.). Elemental composition was determined using the standard less ZAF option Z [atomic number correction related to stopping power of the element]; A [absorption correction (less energetic X-rays from lighter elements are absorbed upon leaving the sample by heavier elements)]; F [fluorescence correction (a more energetic X-ray leaving the sample fluoresces at a lower energy X-ray from lighter elements)].

2.4. Gas chromatography-mass spectrometry

Samples were weighed in a headspace vial in two replicates of 1 g each. Samples were equilibrated at 120°C for 45 min inside the headspace unit of the HS gas chromatography-mass spectrometry (GC-MS), and vapors generated in the headspace vials were swept to a polar 60 m INNOWax capillary column A, (5301 Stevens Creek Blvd, Santa Clara, CA 95051, United States). Components were resolved by temperature programming between 50°C and

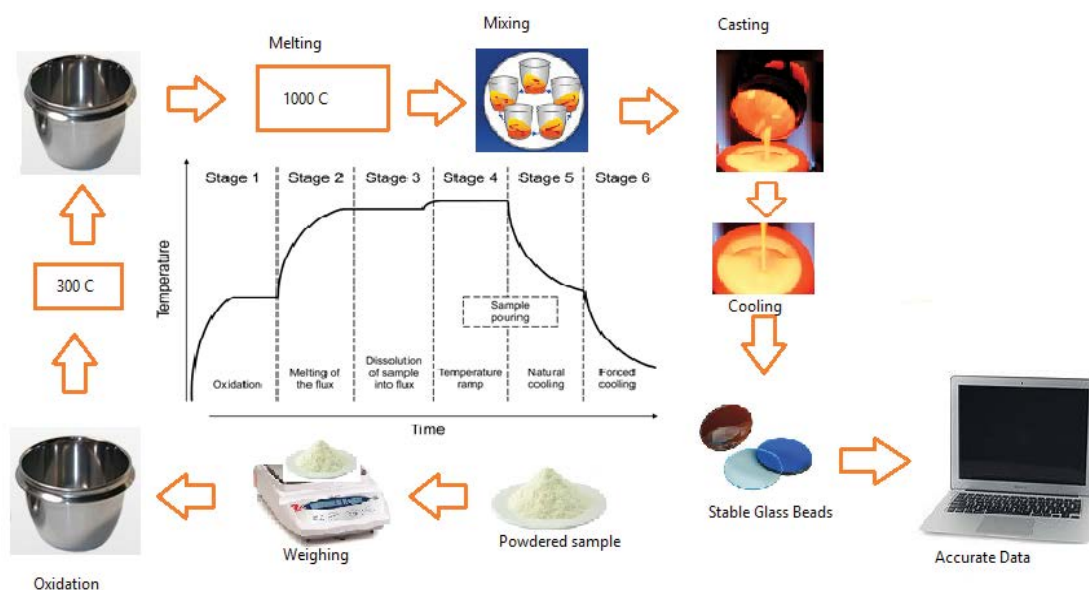


Fig. 2. The procedure was used for preparing glass beads for XRF analysis.

245°C. Compounds were identified by mass spectrometry for m/z between 20 and 650. The identification of the compounds was based on the Wiley Mass Spectral Library with >90% matching factor.

2.5. Adenosine triphosphate C-110 Kikkoman Lumitester

A modified method of the adenosine triphosphate (ATP) hot water extraction [12] was used to extract exogenous and cellular ATP from the samples. The pulverized sample was transferred to a lyophilizer to induce cellular freeze-fracture, arrest potential ATPase activity, and remove moisture. Treated samples were stored in a desiccator, weighed, aspirated, chilled, and then extracted and tested using CheckLite HS Luciferin-Luciferase with a C-110 Kikkoman Lumitester. ATP concentration was determined using a standard concentration curve.

3. Results and discussion

3.1. Deaerator scale

Organic species of scale in the lower part of the deaerator were of moderate molar mass (mostly 6–15 carbon chains), as most low molar mass molecules would be volatile and evolved with non-condensable gases from venting nozzles. Sources of most organic compounds identified could be assigned to; the antifoam agent employed (siloxane-based), degradation products of polysaccharide, and medium-chain fatty acids present in the bacterioneuston (lipid-derived aldehydes and ketones, carbohydrate-derived aldehydes), or common components of the water column (carbon disulfide) Fig. 3. Described are chemical compounds identified in the deaerator scale that exist in seawater.

3.1.1. Carbon disulfide

Carbon disulfide (CS_2) is the only low molecular weight organic compound identified in the deaerator scale. CS_2

is ubiquitous in the atmosphere and sea. In seawater, CS_2 may be from enzymatic oxidation of biopolymers from cyanobacteria and algae [13], photo-oxidation (from sunlight), or chemical oxidation (from industrial processes or anthropogenic discharges). CS_2 may also be a product of anaerobic metabolism generated in salt marsh environments of the Arabian Gulf [14]. Carbon disulfide is a product of enzymatic and photo-oxidation of chromophoric dissolved organic matter (CDOM) [15,16]. Breakdown of S-amino acids is another source for CS_2 in seawater; also, the roots of terrestrial and marine plants that manufacture CS_2 to protect from predators [17].

3.1.2. Aldehydes (lipid-based organics)

Eight aldehydes are identified as associates of the deaerator scale. Saturated aldehydes derived from fatty acid sources (lipids) floating on seawater include hexanal, octanal, nonanal, and decanal.

There are four primary sources for hexanal in seawater. Hexanal aerosols (Table 2) can attach to air humidity that nucleates into rainfall, which transfers to the sea [18]. Algae metabolism is another source of seawater hexanal [19] and mammalian body fluid discharges (from aquatic species or anthropogenic sources). Photo-oxidation of CDOM [20] is also an abundant source of hexanal in seawater [16].

Octanal is present in seaweed and some aquatic and terrestrial plants [21] and involved in plant metabolism [22]. Octanal exists in algal species [22], sea mussels, and fish [23].

Nonanal and decanal are also saturated fatty aldehydes observed in the deaerator scale. Both organic chemicals float on top of seawater and are components of algae [22,24]. They have been found as significant components of the biogenic lake-surface microlayer [25] and part of the sea-surface microlayer in Mediterranean waters with origins attributed to plankton [26].

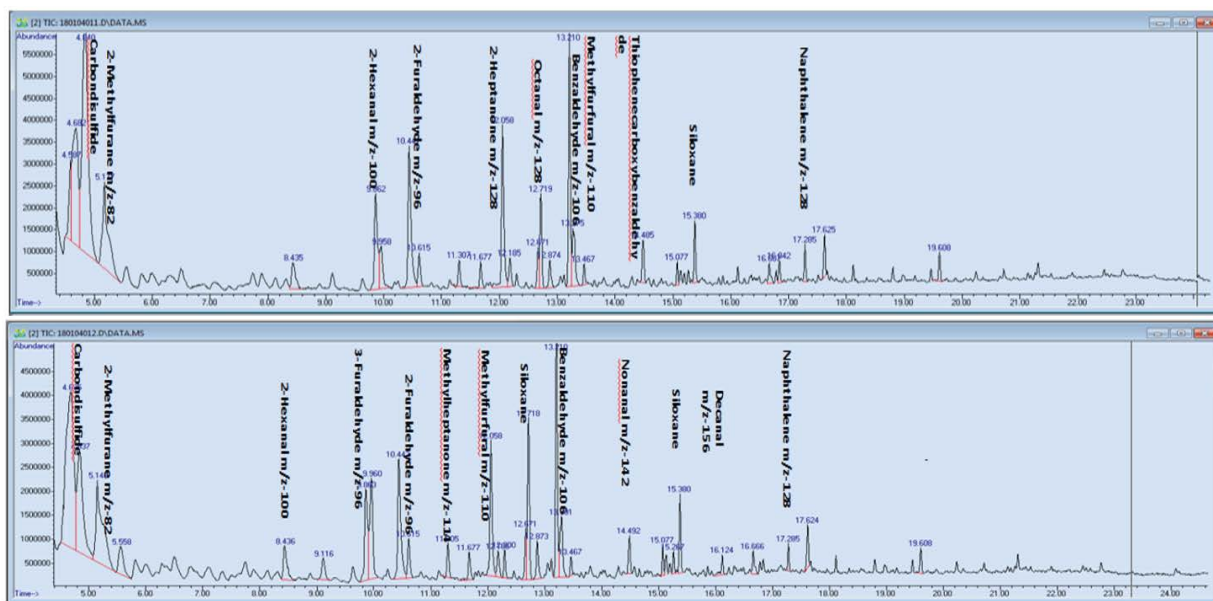


Fig. 3. GC-MS spectrograms of organic component associated with deaerator scale (a) set I and (b) set II.

3.1.3. Ketones (lipid-based organics)

2-Heptanone was also identified as a component of soft scale deposition in MSF deaerators. 2-Heptanone is a potent anti-microbial agent produced by species of seaweed that do not have cell-mediated immune responses [27]. Seaweed manufactures anti-microbial agents as protection against ubiquitous bacteria in the sea. Algae produce several types of heptanone [28] in addition to butanol for protection against microbes [27].

Methyl heptanone is a compound associated with pheromones of some aquatic species. It also presents in bacillus bacteria that aids in the arrest of cyanobacterial blooms [29,30].

Methyl heptanone is identified as part of the deaerator soft-scale of an Arabian Gulf MSF desalination co-generation plant.

3.1.4. Aldehyde (carbohydrate-based organics)

Methyl furfural, identified in scale, is a component of algae [31]. This aldehyde is involved in protein oxidation and inhibition, oxygen scavenging, and is a detoxifying antioxidant [32].

2-Furaldehyde and its 3-furaldehyde isomer are breakdown by-products of cellulose and biological inhibitors of many fermenting organisms. Though there are numerous speculative sources of furfurals in seawater (i.e., anthropogenic discharge, municipal discharge, mangroves, oil, and gas extraction, oil spills), however, there is no direct correlation associating their presence in deaerator-scales.

Of the aldehydes associated with soft scale formation in the deaerator decanal, nonanal and octanal exist throughout epilithic biofilms and within their (the biofilms) mineralized layer. These lipid-based aldehydes are observed in marine biofilms manufactured by cyanobacteria phylotypes; *C. parietina*, *Calothrix* sp., *Plectonema* sp., *Phormidium* sp., *T. distorta*,

Rivularia sp. [33], and the *P. notatum* fungus. Decanal, nonanal, and octanal are important metabolites for cyanobacteria that were responsible for metabolic clean-up of the world's most massive oil spill occurring in the 1991 Arabian Gulf War [33,34].

2-Heptanone is a lipid-based ketone that is also a metabolite of cyanobacteria. It is also a part of epilithic biofilms. However, it is not associated with the encrusted biofilm, and its association with biological species has yet to be confirmed [33].

3.2. Flash chamber scale

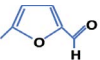
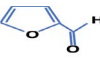
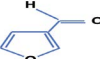


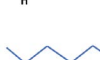
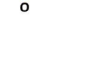

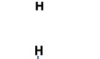


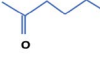
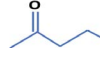
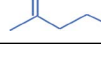
Within the first stage flash chamber, only lipid-based compounds were found in scales (Fig. 4). Several ketone compounds are discovered and one aldehyde. Carbohydrate-derived species did not present in the scale of the MSF flash chamber, which we provisionally attribute to their greater water-solubility.

3.2.1. Ketones

2-Decanone is one of several organic compounds related to scale in the flash chamber. 2-Decanone is a plant metabolite associated with epilithic biofilms found in the encrusted layer [33]. 2-Decanone is identified in red algae like *Laurencia brandenii* (found in the Arabian Gulf and South West Coast of India) for its biocidal activity in the control of microbial biofilms [35]. 2-Decanone's existence in the encrusted layer of biofilms necessitates further investigation into its presence and role in microbial chemistry and scale formation.

Another component identified as part of the MSF flash chamber scale is 2-Nonanone, a compound present in many fruits, vegetables, and nuts. 2-Nonanone is associated with nematicides of soil bacteria [36] and biofilm from a marine microorganism [37].

Table 2
Organic compounds associated with scales of the deaerator and flash chamber of a commercial MSF Plant (located on the Arabian Gulf)

	Structure	Compound	Boiling Point (°C)	Solubility in water (g/L)	Density (g/cm ³)
Carbohydrate-based organics		5-Methylfurfural	187.0	29.100	1.107
		2-Furaldehyde (furfural)	161.7	83.000	1.160
		3-Furaldehyde	145.3	44.000	1.110
		Nonanal (nonyl aldehyde)	191.0	0.060	0.830
		Decanal	83.0	0.008	0.830
		2-Heptanone	126.0	4.210	0.800
Lipid-based organics		Methyl-heptanone	151.0	2.260	1.480
		Hexanal	131.0	4.800	0.815
		Octanal	171.0	0.560	0.821
		Nonanal	191.0	0.132	0.827
		Decanone	208.5	0.008	0.83
		2-Heptanone	151.0	4.210	0.800
		6-Methyl-2-heptanone	167.0	1.370	0.816
		3-Heptanone			

3-Octanone was identified in the flash chamber scale. Amyl ethyl ketone is a constituent of micro-fungi of aquatic biofilms [37] present in axenic benthic cyanobacteria [38].

3-Heptanone was also identified as a component of the flash chamber scale. It is commonly used as a dispersant. 3-Heptanone is found in seawater and can undergo photo-oxidation to be associated with seawater smog formation [39]. 3-heptanone exists in nereidid polychaetes found in coastal seawaters.

3.2.2. Alkanes

2-Nonadecane was the only alkane found to be associated with the scale of the first stage flash chamber. Nonadecane is identified as a component of green-brown seaweed like

H. filicina, algae, and seagrass of the Mediterranean, Red Sea, and Arabian Gulf [40].

3.3. ATP results

ATP is associated with scale in the deaerator and flash chamber. In the deaerator, concentrations were in the range of 3.62×10^3 RLU/g (three orders of magnitude) corresponding to 1.698×10^4 pM/g of ATP. Within the flash chamber, ATP was detected as a component of the cellular scale. Its RLU value was one order of magnitude less than that of the deaerator (4.32×10^1 RLU/g) corresponding to a total ATP concentration of 2.03×10^2 pM/g. It is unclear if the source of ATP is exogenous or intracellular.

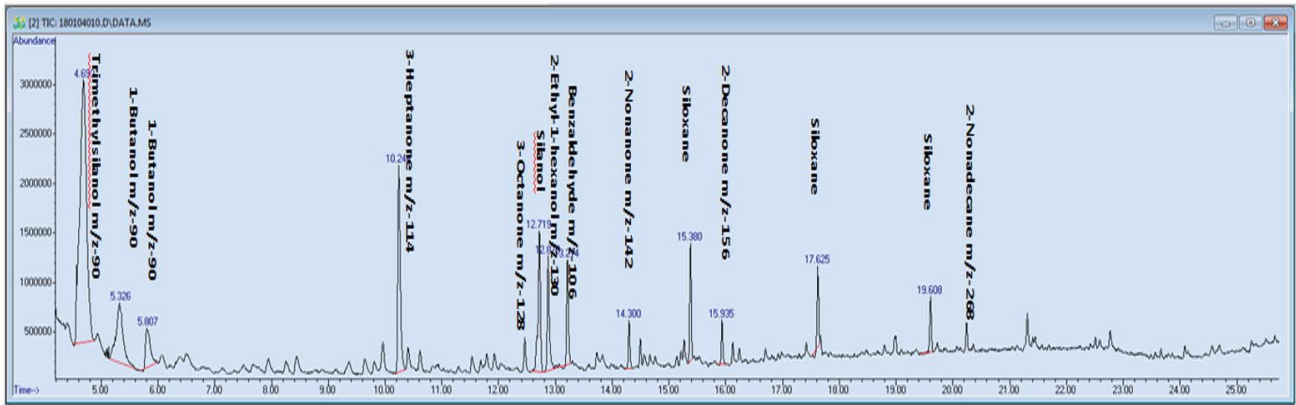


Fig. 4. GC-MS spectrograms of organic component associated with the first stage flash chamber.

The presence of ATP in the deaerator is not unusual. The temperature range of the deaerator system is reflective of seawater ambient temperature conditions. The presence of ATP associated with the flash chamber scale is exciting, leading to the possibility of scale intercalating organisms within a crystal matrix. This hypothesis necessitates further investigations.

3.4. Inorganics of scale

3.4.1. Deaerator scale

The SEM micrographs of the deaerator scale show the presence of bivalves in the larval stage, scale agglomerates, and a background that is biofilm (Fig. 5a). EDX reveals an environment predominantly comprised of magnesium, calcium, and oxygen, with calcium carbonate and magnesium hydroxide likely to be the main species (Fig. 5a). While the temperature at the deaerator (~40°C) should lead to the formation of calcium carbonate over magnesium

hydroxide [3], it has been shown that the initial layer of deposition of soft scale is typically magnesium hydroxide at lower temperatures [41], due to the increased pH of the interfacial microenvironment. Findings are consistent with the SEM image, which appears to show a background of fine magnesium hydroxide crystals with larger calcium carbonate deposits on top- similar to the observations of Wildebrand et al. [40]. EDX analysis of the scale did not reveal any products that could result, in principle, from corrosion of thermal systems (copper, nickel, chromium, titanium), with exception to small iron peaks- due to lower concentration detection inefficiencies of the EDX technique. The small aluminum and silica peaks in EDX may indicate a minor component of clay or diatomaceous silica in scale. The minor peak assigned to sulfur may arise from organic sulfur species identified above or sulfate salt formed on the evaporation of residual seawater of the sample.

The XRF results (shown in Table 3) reveal the presence of iron (5.84E+03 ppm), perhaps attributed to corrosion

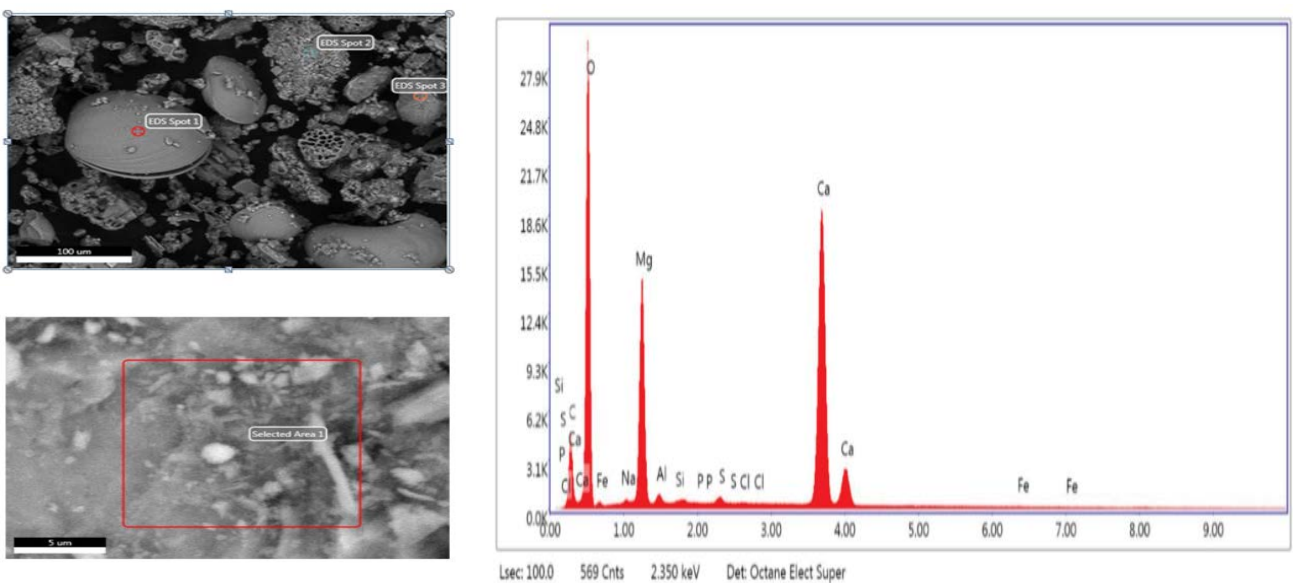


Fig. 5. (a) SEM and (b) EDX of scale samples of the MSF deaerator.

Table 3
The metal concentration measured by using XRF

Sample	Ca (ppm)	Na (ppm)	Mg (ppm)	Fe (ppm)	Mn (ppm)	Al (ppm)
Deaerator-(sample set I)	2.27E+05	1.65E+04	1.28E+04	5.55E+03	1.01E+02	6.55E+03
Deaerator-(sample set II)	2.31E+05	1.61E+04	1.38E+04	6.12E+03	1.15E+02	6.02E+03
Average	2.29E+05	1.63E+04	1.33E+04	5.84E+03	1.08E+02	6.29E+03
Standard deviation (STDEV)	2.83E+03	2.80E+02	7.10E+02	4.01E+02	9.47E+00	3.74E+02
Relative standard deviation (RSD%)	1.24E+04	1.74E+04	5.32E+04	6.86E+00	8.78E+00	5.95E+00
Flash chamber-(sample set I)	3.31E+04	1.20E+03	3.49E+05	2.25E+02	4.50E+00	2.60E+02
Flash chamber-(sample set II)	3.29E+04	1.20E+03	3.49E+05	2.05E+02	4.60E+00	2.52E+02
Average	3.30E+04	1.20E+03	3.49E+05	2.15E+02	4.55E+00	2.56E+02
Standard deviation (STDEV)	1.40E+02	0.00E+00	2.10E+02	1.39E+01	7.10E-02	5.37E+00
Relative standard deviation (RSD%)	4.30E+03	0.00E+00	6.00E+02	6.49E+00	1.55E+00	2.10E+00

products in the system and aluminum from clay and corrosion products. Calcium ($2.29E+05$ ppm) has a higher average concentration than magnesium ($1.33E+04$ ppm) in scale, reflecting a predominance of calcium carbonate formation over magnesium hydroxide. Results are thermodynamically consistent with scale formation in the deaerator that is confirmed by EDX results (Fig. 5b). The presence of magnesium hydroxide in the deaerator at temperatures lower than 80°C may be due to the purging of non-condensable gases from the seawater feed during deaeration.

3.4.2. Flash chamber

The SEM and EDX results obtained from scale formed in the first flash chamber (Fig. 6) are consistent with a continuous layer of magnesium hydroxide crystals (Fig. 6) the expected alkaline scale product at the temperature of $\sim 100^{\circ}\text{C}$ prevailing in the flash chamber, with a minimal amount of calcium carbonate. EDX analysis again did not show peaks attributable to possible corrosion products, with a

possible exception of iron. Minor peaks of aluminum and silica are attributed to clay or diatomaceous silica and sulfur (possibly arising from small calcium sulfate components).

The XRF results confirm the findings of SEM and EDX. Magnesium and calcium have the highest concentrations ($3.49E+05$ ppm and $3.30E+04$ ppm, respectively [Table 3]), indicating that magnesium hydroxide and calcium carbonate are the more significant components of scale, respectively. EDX results confirmed this finding. XRF reveals products that could result from corrosion of thermal systems (manganese and titanium) due to its low detection limits.

4. Conclusion

Organic compounds associated with scale formation were identified in the deaerator and beginning stage flash chamber of a commercial MSF desalination facility located on the Arabian Gulf. In the deaerator, medium-chain carbohydrate and lipid aldehydes and ketones are observed. Carbon disulfide, a ubiquitous sea, and the atmospheric

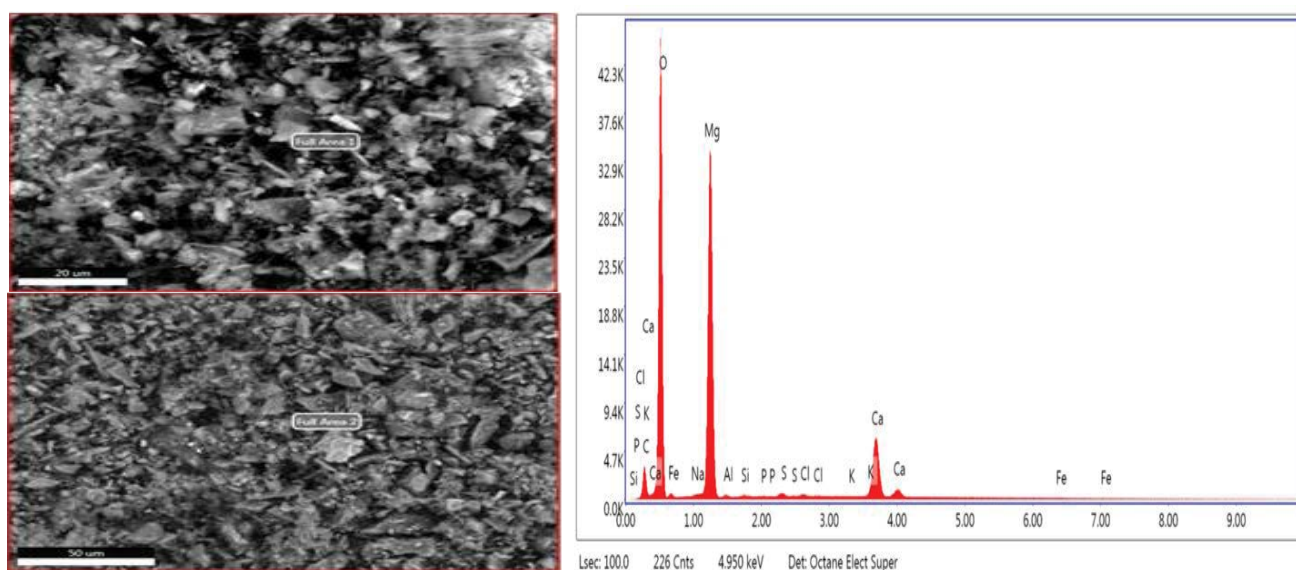


Fig. 6. (a) SEM and (b) EDX of scale samples of the MSF flash chamber.

compound were also found as part of the soft scale matrix. Scales associated with the flash chamber are mostly magnesium hydroxide.

Organic compounds associated with flash chamber scales are lipid-based aldehydes and ketones. No carbohydrate intercalates are identified. It is important to note that nearly all organic compounds associated with scales can be related to aquatic species in the sea. It is therefore highly probable that organic compounds related to scale may have originated from marine sources.

Scales associated with the deaerator contains copious amounts of ATP. ATP is nearly one order of magnitude higher in the deaerator scale than scales of the flash chamber. Given the process of high-temperature vaporization of seawater in flash chambers to produce potable water, the presence of ATP in scale likely indicates biotic intercalation or activity in the flash chamber scale. Such finding is exciting and warrants further investigation.

Inorganic analysis of scale is consistent with the thermodynamic profiles of the deaerator and flash chamber. X-ray diffraction (XRD) and XRF analysis reveal calcium and magnesium in scale corresponding to calcium carbonate and magnesium hydroxide. In the deaerator, calcium carbonate is the dominant species of scale. In the flash chamber, XRD and XRF indicate that magnesium hydroxide is dominant in scale, which is thermodynamically consistent. Also, corrosion product intercalated in scale is found in the deaerator and flash chamber. The presence of carbon and high oxygen signals in XRD for both the deaerator and the flash chamber may also be indicative of organics in scale.

Research indicating the role of organics in the nucleation of scale is essential to the understanding of scale formation and mitigation in industrial environments. It is, therefore, necessary for industries to consider the role of micro- and macro-organisms, organic compounds, and chemical additives in process applications not only for biological fouling but also scale formation. As indicated in the different chemical composition of organics in the deaerator and flash chamber, temperature plays a role in preference of organics favored in scale (lipid-based vs. carbohydrate-based organics). What is novel is the understanding that in thermal desalination processes, the temperature does not exclude living organisms or its biotic materials from participating in the nucleation and growth of scale.

References

- [1] The World Bank, The Role of Desalination in an Increasingly Water Scarce World, Global Water Security, and Sanitation Partnership (GWSP), 2019. Available at: www.worldbank.org
- [2] J.X. Lu, K. Foster, J. Murray, Biochemistry, Dissolution and Solubility, StatPearls Publishing, Florida, 2019.
- [3] A. Alhamzah, C.M. Fellows, Apparent inhibition of thermal decomposition of hydrogencarbonate ion by poly(acrylic acid). The effect of molar mass and end-group functionality, *Desalination*, 332 (2014) 33–43.
- [4] A.M. Shams El Din, R.A. Mohammed, Brine and scale chemistry in MSF distillers, *Desalination*, 99 (1994) 73–111.
- [5] D. Hasson, M. Avriel, W. Resnick, T. Rozenman, S. Windreich, Mechanism of calcium carbonate scale deposition on heat-transfer surfaces, *Ind. Eng. Chem. Fundam.*, 7 (1968) 59–65.
- [6] R.A. Dawe, Y.P. Zhang, Kinetics of calcium carbonate scaling using observations from glass micromodels, *J. Pet. Sci. Eng.*, 18 (1997) 179–187.
- [7] T. Østvold, P. Randhol, Kinetics of CaCO₃ Scale Formation. The Influence of Temperature, Supersaturation and Ionic Composition, Society of Petroleum Engineers, International Symposium on Oilfield Scale, 30–31 January, Aberdeen, United Kingdom, 2001.
- [8] S.F.E. Boerlage, Scaling and Particulate Fouling in Membrane Filtration Systems, Balkema Publishers, Netherlands, 2001.
- [9] P.G. Vekilov, Two-step mechanism for the nucleation of crystals from solution, *J. Cryst. Growth*, 275 (2005) 65–76.
- [10] S. Basu, A.K. Debnath, Chapter II – Main Equipment, S. Basu, A.K. Debnath, Eds., Power Plant Instrumentation and Control Handbook: A Guide to Thermal Power Plants, Academic Press, Boston, 2015, pp. 39–146.
- [11] P.K. Abdul Azis, I. Al-Tisan, M. Al-Daili, T.N. Green, A.G.I. Dalvi, M.A. Javeed, Effects of environment on source water for desalination plants on the eastern coast of Saudi Arabia, *Desalination*, 132 (2000) 29–40.
- [12] N.-C. Yang, W.-M. Ho, Y.-H. Chen, M.-L. Hu, A convenient one-step extraction of cellular ATP using boiling water for the luciferin–luciferase assay of ATP, *Anal. Biochem.*, 306 (2002) 323–327.
- [13] D.P. Kelly, A.P. Wood, S.L. Jordan, A.N. Padden, V.M. Gorlenko, G.A. Dubinina, Biological production and consumption of gaseous organic sulfur compounds, *Biochem. Soc. Trans.*, 22 (1994) 1011–1015.
- [14] V.P. Aneja, J.H. Overton, L.T. Cupitt, J.L. Durham, W.E. Wilson, Carbon disulfide and carbonyl sulfide from biogenic sources and their contributions to the global sulfur cycle, *Nature*, 282 (1979) 493–496.
- [15] N.B. Nelson, D.A. Siegel, The global distribution and dynamics of chromophoric dissolved organic matter, *Annu. Rev. Mar. Sci.*, 5 (2011) 447–476.
- [16] S.T. Lennartz, M. von Hobe, D. Booge, H.C. Bittig, T. Fischer, R. Gonçalves-Araujo, K.B. Ksionzek, B.P. Koch, A. Bracher, R. Röttgers, B. Quack, C.A. Marandino, The influence of dissolved organic matter on the marine production of carbonyl sulfide (OCS) and carbon disulfide (CS₂) in the Peruvian upwelling, *Ocean Sci.*, 15 (2019) 1071–1090.
- [17] W.L. Banwart, J.M. Bremner, Formation of volatile sulfur compounds by microbial decomposition of sulfur-containing amino acids in soils, *Soil Biol. Biochem.*, 7 (1975) 359–364.
- [18] D. Balla, A. Papageorgiou, D. Voutsas, Carbonyl compounds and dissolved organic carbon in rainwater of an urban atmosphere, *Environ. Sci. Pollut. Res. Int.*, 21 (2014) 12062–12073.
- [19] K. Boonprab, K. Matsua, M. Yoshida, Y. Akakabe, A. Chirapart, T. Kajiwara, C6-aldehyde formation by fatty acid hydroperoxide lyase in the brown alga *Laminaria angustata*, *Z. Naturforsch., C: Biosci.*, 58 (2003) 207–214.
- [20] R.J. Kieber, L.H. Hydro, P.J. Seaton, Photooxidation of triglycerides and fatty acids in seawater: implication toward the formation of marine humic substances, *Limnol. Oceanogr.*, 42 (1997) 1454–1462.
- [21] Y.-S. Seo, H.-N. Bae, S.-H. Eom, K.-S. Lim, I.-H. Yun, Y.-H. Chung, J.-M. Jeon, H.-W. Kim, M.-S. Lee, Y.-B. Lee, Y.-M. Kim, Removal of off-flavors from sea tangle (*Laminaria japonica*) extract by fermentation with *Aspergillus oryzae*, *Bioresour. Technol.*, 121 (2012) 475–479.
- [22] I. Jerkovic, M. Kranjac, Z. Marijanovic, M. Roje, S. Jokić, Chemical diversity of headspace and volatile oil composition of two brown algae (*Taonia atomaria* and *Padina pavonica*) from the Adriatic Sea, *Molecules*, 24 (2019) 495, doi: 10.3390/molecules24030495.
- [23] T. Cserhádi, E. Forgács, FLAVOR (FLAVOUR) COMPOUNDS: Structures and Characteristics, B. Caballero, Ed., Encyclopedia of Food Sciences and Nutrition, Academic Press, Oxford, 2003, pp. 2509–2517.
- [24] X.-W. Chen, Y.-J. Chen, J.-M. Wang, J. Guo, S.-W. Yin, X.-Q. Yang, Phytosterol structured algae oil nanoemulsions and powders: improving antioxidant and flavor properties, *Food Funct.*, 7 (2016) 3694–3702.
- [25] A. Dąbrowska, J. Nawrocki, E. Szeląg-Wasielewska, Appearance of aldehydes in the surface layer of lake waters, *Environ. Monit. Assess.*, 186 (2014) 4569–4580.

- [26] P. Astrahan, Monocyclic aromatic hydrocarbons (phthalates and BTEX) and aliphatic components in the SE Mediterranean coastal sea-surface microlayer (SML): origins and phase distribution analysis, *Mar. Chem.*, 205 (2018) 56–69.
- [27] M.J. Pérez, E. Falqué, H. Domínguez, Antimicrobial action of compounds from marine seaweed, *Mar. Drugs*, 14 (2016) 52–61.
- [28] R.S. Beissner, W.J. Guilford, R.M. Coates, L.P. Hager, Synthesis of brominated heptanones and bromoform by a bromoperoxidase of marine origin, *Biochemistry*, 20 (1981) 3724–3731.
- [29] T. Lee, D. Park, K. Kim, S.M. Lim, N.H. Yu, S. Kim, H.-Y. Kim, K.S. Jung, J.Y. Jang, J.-C. Park, H.H. Ham, S.H. Lee, S.K. Hong, J.-C. Kim, Characterization of *Bacillus amyloliquefaciens* DA12 showing potent antifungal activity against mycotoxigenic *Fusarium* species, *Plant Pathol. J.*, 33 (2017) 499–507.
- [30] J. Yu, Y. Kong, S.Q. Gao, L.H. Miao, P. Zou, B. Xu, C. Zeng, X.L. Zhang, *Bacillus amyloliquefaciens* T1 as a potential control agent for cyanobacteria, *J. Appl. Phycol.*, 27 (2015) 1213–1221.
- [31] T. Levring, H.A. Hoppe, O.J. Schmid, *Marine Algae: A Survey of Research and Utilization*, Botanica Marina Handbooks, Cram, deGruyter and Co., Hamburg, 1969.
- [32] Y.-X. Li, Y. Li, Z.J. Qian, M.-M. Kim, S.-K. Kim, In vitro antioxidant activity of 5-HMF isolated from marine red alga *Laurencia undulata* in free-radical-mediated oxidative systems, *J. Microbiol. Biotechnol.*, 19 (2009) 1319–1327.
- [33] C. Höckelmann, T. Moens, F. Jüttner, Odor compounds from cyanobacterial biofilms acting as attractants and repellents for free-living nematodes, *Limnol. Oceanogr.*, 49 (2004) 1809–1819.
- [34] H.J. Barth, The influence of cyanobacteria on oil polluted intertidal soils at the Saudi Arabian Gulf shores, *Mar. Pollut. Bull.*, 46 (2003) 1245–1252.
- [35] A. Manilal, S. Sujith, G. Seghal Kiran, J. Selvin, C. Shakir, Cytotoxic potentials of red alga, *Laurencia brandenii* collected from the Indian Coast, *Global J. Pharmacol.*, 3 (2009) 90–94.
- [36] Y.-Q. Gu, M.-H. Mo, J.-P. Zhou, C.-S. Zou, K.-Q. Zhang, Evaluation and identification of potential organic nematocidal volatiles from soil bacteria, *Soil Biol. Biochem.*, 39 (2007) 2567–2575.
- [37] I. Skjevraak, V. Lund, K. Ormerod, H. Herikstad, Volatile organic compounds in natural biofilm in polyethylene pipes supplied with lake water and treated water from the distribution network, *Water Res.*, 39 (2005) 4133–4141.
- [38] C. Höckelmann, F. Jüttner, Volatile organic compound (VOC) analysis and sources of limonene, cyclohexanone and straight chain aldehydes in axenic cultures of *Calothrix* and *Plectonema*, *Water Sci. Technol.*, 49 (2004) 47–54.
- [39] J.L. O'Donoghue, *Ketones of Six to Thirteen Carbons*, Patty's Toxicology, Rochester, 2012, pp. 807–914.
- [40] I. Jerković, Z. Marijanović, M. Roje, P.M. Kuš, S. Jokić, R. Čož-Rakovac, Phytochemical study of the headspace volatile organic compounds of fresh algae and seagrass from the Adriatic Sea (single point collection), *PLoS One*, 13 (2018), <https://doi.org/10.1371/journal.pone.0196462>.
- [41] C. Wildebrand, H. Glade, S. Will, M. Essig, J. Rieger, K.-H. Büchner, G. Brodt, Effects of process parameters and anti-scalants on scale formation in horizontal tube falling film evaporators, *Desalination*, 204 (2006) 448–463.